Estimation Method for Rotor Eddy Current Loss in Ultrahigh-Speed Surface-Mounted Permanent Magnet Synchronous Motor

Dong-Min Kim[1], Jae-Hyun Kim[1], Soo-Gyung Lee[1], Min-Ro Park[2], Geun-Ho Lee[3], and Myung-Seop Lim[1]

[1]Department of Automotive Engineering, Hanyang University, Seoul 04763, South Korea
[2]Interactive Robotics R&D Division, Korea Institute of Robotics & Technology Convergence, Pohang 37666, South Korea
[3]Graduate School of Automotive Engineering, Kookmin University, Seoul 02707, South Korea

Surface-mounted permanent magnet synchronous motors (SPMSMs) usually adopt a retaining sleeve for ultrahigh-speed (UHS) applications. The retaining sleeve usually has high electrical conductivity and cannot be segmented. Accordingly, the rotor eddy current loss is high. Moreover, the higher the eddy current loss, the higher is the rotor temperature. Therefore, the rotor eddy current loss should be considered in the design stage. However, the eddy current loss is generally calculated through three-dimensional finite-element analysis (3-D FEA) and considered cumbersome because of the high computation time. This article proposes a simple estimation method for the rotor eddy current loss of a UHS SPMSM according to the motor size. In this study, the mechanically stable cross-sectional structure of the rotor was fixed, and a formula for predicting the eddy current loss of the rotor based on motor size was devised. In this method, the basic electromagnetic formula for eddy current and the frozen permeability method were utilized. The proposed method was validated via comparisons with the results of 3-D FEA.

Index Terms— **Eddy current loss, fuel cell electric vehicle, surface-mounted permanent magnet synchronous motor (SPMSM), ultrahigh-speed (UHS) motor.**

I. Introduction

THE fuel cell stack of a fuel cell electric vehicle needs oxygen supply at high flow rate and high pressure. Hence, an electric-motor-driven centrifugal air compressor is adopted. A surface-mounted permanent magnet synchronous motor (SPMSM) is generally used for this application. Furthermore, because of the ultrahigh-speed (UHS) operating condition, a retaining sleeve is essential. However, the retaining sleeve has electrical conductivity, and hence, eddy current loss is inevitable. Therefore, in the design of a UHS SPMSM, mechanical stability and loss distribution must be considered.

The design process of a UHS SPMSM generally includes the following aspects.

1) Considering the mechanical stress, the size of the rotor is determined.

2) Considering the total loss, the overall size of the motor is determined.

The second step should include the estimation of the total loss according to the motor size. Particularly, the eddy current loss in the sleeved rotor accounts for a high proportion of the total loss and it directly affects the residual induction of the permanent magnet (PM) because of temperature rise. Therefore, the loss distribution including the rotor eddy current loss should be determined in the design of a UHS SPMSM. However, the calculation of the eddy current loss requires a high computation time.

Manuscript received May 6, 2020; revised August 22, 2020; accepted October 9, 2020. Date of publication October 13, 2020; date of current version January 20, 2021. Corresponding author: M.-S. Lim (e-mail: myungseop@hanyang.ac.kr).

Color versions of one or more of the figures in this article are available online at https://ieeexplore.ieee.org.

Digital Object Identifier 10.1109/TMAG.2020.3030684

Several studies have been conducted on rotor eddy current loss for a UHS motor. Recently, Hannon *et al*. [1] reduced the rotor eddy current loss using a shielding cylinder. They studied the effect of the thickness and conductivity of the shielding cylinder on the reduction of the rotor eddy current loss. However, it is difficult to use this method in a UHS motor design process. Zhang *et al.* [2] suggested an analytical model to evaluate the rotor eddy current loss. Their model showed high accuracy for various speed conditions. However, it is difficult to use this model to determine the motor size, as it does not consider the permeability of the core.

This article proposes an estimation method for the rotor eddy current loss according to the overall motor size. This method estimates the rotor eddy current loss based on the 3-D finite-element analysis (3-D FEA) result of the baseline. Accordingly, the eddy current loss is separated into two terms using the frozen permeability method. Then, the eddy current loss is estimated for various stack lengths and motor volumes. Finally, the proposed method is validated by comparing it with the results of 3-D FEA.

The contributions of the proposed method for estimating the rotor eddy current loss are as follows:

1) Suggestion of a simple estimation formula.
2) Achievement of high accuracy with low computation time.
3) Determination of the tendency of eddy current loss according to the motor size.

II. Base Model

The maximum requested output power of an electric motor is 15 kW at the rotational speed of 110 kRPM. Due to this UHS operating condition, an SPMSM having a retaining sleeve

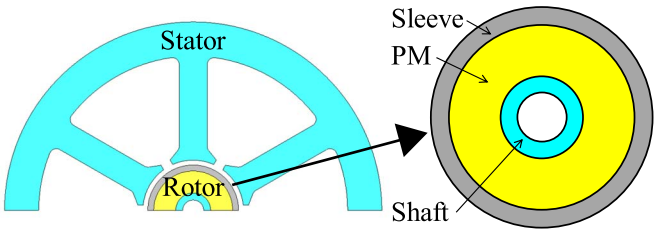

Fig. 1. Structure of the target UHS motor.

TABLE I
SPECIFICATIONS OF THE BASE MODEL

Parameters	Value	Unit
Pole / Slot	2 / 6	-
Stator diameter	92	mm
Stack length	56	mm
Maximum rotational speed	110	kRPM
Maximum output power	15	kW

structure was adopted to prevent the scattering of the PM. Moreover, a centered air hole was adopted to reduce the temperature rise of the rotor caused by the rotor eddy current loss. The construction of the base model is depicted in Fig. 1. As shown in Fig. 1, the slot number was determined as six with concentrated windings, to minimize the end coil height. Such a short-end coil allows the journal bearings to be closer to each other. Consequently, greater rotational stability can be secured [3]. Moreover, to supply a sinusoidal waveform of the input current, the pole number was minimized to two because of the UHS condition. In Table I, the specifications of the base model are listed. The materials used in the rotor are Sm_2Co_{17} for the PM, Inconel 718 for the retaining sleeve, and STS630 for the rotor core.

In this study, the eddy current loss of the rotor was investigated according to the stator size. During the examination, the cross-sectional structure of the rotor was fixed; and the radii of the retaining sleeve, PM, and rotor core were fixed. The mechanical stability of the base model of this rotor was validated using structural FEA and fabricated sample tests. As shown in Fig. 2, a prototype of the air compressor with the base model was fabricated.

Using this prototype, an air compression test was conducted. The setup for this test is shown in Fig. 3. This setup consisted of a dc power supply, inverter, oscilloscope, power analyzer, thermocouple, mass flow sensors, and gas pressure sensors. Moreover, a chiller for the water-cooling channel was installed. Using this experimental setup, the compression ratio and outlet temperature were measured and depicted in Fig. 4. Moreover, estimated torque was depicted in Fig. 4, as blue bar. This torque was assumed based on torque coefficient and measured current considering PM temperature. At the maximum speed, the desired air compressor performance was confirmed. Also, it can be assumed that the UHS SPMSM for air compressor achieved target output power.

Consequently, the mechanical stability of the rotor was validated for the 110 kRPM. As the temperature affects the mechanical characteristics of each rotor material differently,

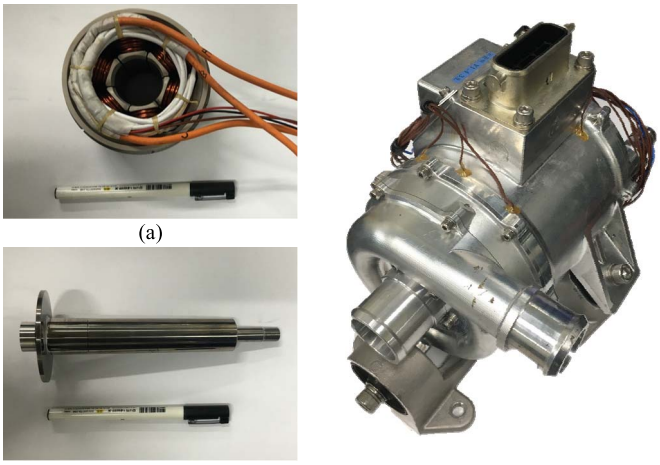

Fig. 2. Prototype of the base model (a) stator, (b) rotor, and (c) compressor assembly.

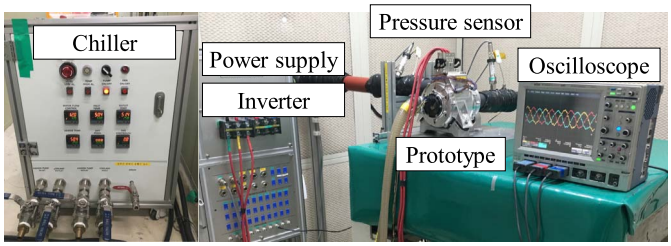

Fig. 3. Experiment setup for air compression test.

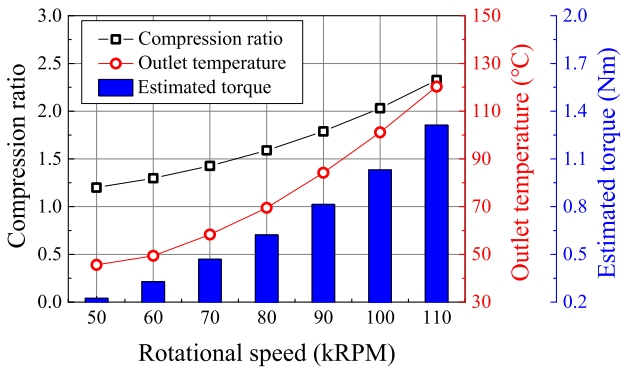

Fig. 4. Air compression test results for the prototype air compressor.

the operating temperature range is considered for the mechanical stability analysis of the rotor. In this article, the possible minimum temperature was assumed to be −40 °C and the maximum temperature to be 160 °C. In Table II, the material properties of the rotor are listed. Using these mechanical properties, 2-D structural FEA was performed using ANSYS with an additional rotational speed of 15% of the maximum. This FEA result is listed in Table III. The safety factor from failure theory was more than 1.3 for all the conditions and materials. At this time, the von Mises and modified Mohr theories were applied to calculate the safety factors of the retaining sleeve and PM [4].

III. EDDY CURRENT LOSS ESTIMATION

A. Estimation Condition

The eddy current loss of the rotor was estimated from the experimentally validated base model according to the change

TABLE II
ROTOR MATERIAL PROPERTIES

Items	Retaining sleeve	Permanent magnet	Shaft
Density (kg/m^3)	8190	8400	7750
Yield strength (MPa)	1036	42*/900**	1000
Young's modulus (GPa)	211	151	196
Poisson's ratio	0.29	0.27	0.27
***CTE (10^{-6}/℃)	13.5	9.6	10.8
Electric conductivity (S/m)	0.83×10^6	1.25×10^6	-

*tensile / **compressive / ***coefficient of thermal expansion

TABLE III
ROTOR STRUCTURAL FEA RESULT FROM ANSYS AT 126.5 kRPM

Temperature	Retaining sleeve Max. von Mises stress (safety factor)	Permanent magnet principal stress *a*, *b* (safety factor)
-40 °C	787.9 MPa (1.3)	0.0 MPa, -73.4 MPa (12.3)
160 °C	649.4 MPa (1.6)	30.0 MPa, -4.4 MPa (1.4)

in the stack length. The upper boundary of the stack length was determined considering the first bending mode of the rotor. The no-load back electromotive force (EMF) was fixed. Consequently, the number of armature turns according to the stack length can be expressed as (2) based on (1)

$$E \propto L_{\text{stk}} \tag{1}$$

$$N^{\text{Modi.}} = N^{\text{Base}} \frac{L_{\text{stk}}^{\text{Base}}}{L_{\text{stk}}^{\text{Modi.}}}. \tag{2}$$

Here, E is the back EMF, L_{stk} is the stack length, N is the number of armature turns, and the superscripts Base and Modi. represent the base and modified models, respectively. Therefore, the input current I generating the same torque is the same for various stack lengths as shown as follows:

$$I^{\text{Modi.}} = I^{\text{Base}}. \tag{3}$$

Overall, the magnetomotive force (MMF) from the armature coil for the modified model can be expressed as

$$\begin{aligned} \text{MMF}_{\text{Arm.}}^{\text{Modi.}} &= N^{\text{Modi.}} I^{\text{Modi.}} \\ &= N^{\text{Base}} \frac{L_{\text{stk}}^{\text{Base}}}{L_{\text{stk}}^{\text{Modi.}}} I^{\text{Modi.}} \\ &= N^{\text{Base}} I^{\text{Base}} \frac{L_{\text{stk}}^{\text{Base}}}{L_{\text{stk}}^{\text{Modi.}}} \\ &= \text{MMF}_{\text{Arm.}}^{\text{Base}} \frac{L_{\text{stk}}^{\text{Base}}}{L_{\text{stk}}^{\text{Modi.}}}. \end{aligned} \tag{4}$$

The MMF from the PM is constant according to the stack length as shown as follows:

$$\text{MMF}_{\text{PM}}^{\text{Modi.}} = \text{MMF}_{\text{PM}}^{\text{Base}} = \text{constant}. \tag{5}$$

For this estimation, the PM temperature was assumed as 160 °C, which is the highest temperature from the experiment result.

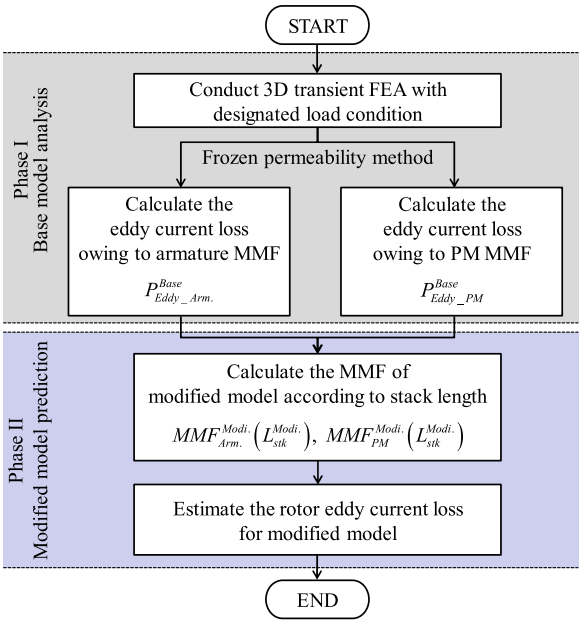

Fig. 5. Proposed method for estimating the eddy current loss of the rotor.

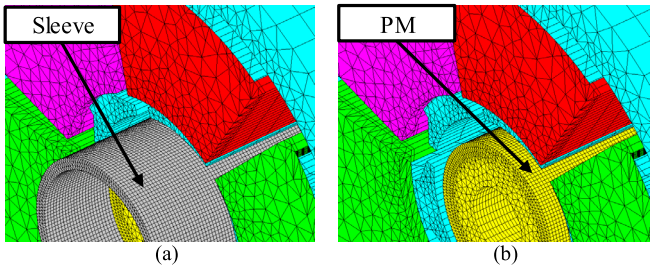

Fig. 6. Generated mesh for the 3-D FEA of (a) sleeve and (b) PM.

B. Estimation Process

This section describes the proposed estimation process as illustrated in Fig. 5. The first step of the proposed method is the calculation of the eddy current loss of the rotor for the base model using 3-D transient FEA. For an accurate analysis, the mesh size of the rotor was determined considering the skin depth δ [5]. Furthermore, the harmonic component was reflected in the skin depth calculation through (6), where μ is the magnetic permeability, n is the desired harmonic order, f is the frequency of the target speed, and σ is the electric conductivity. Fig. 6 shows the mesh size of the rotor considering skin depth as

$$\delta = \frac{1}{\sqrt{\mu \pi n f \sigma}}. \tag{6}$$

Subsequently, the eddy current loss was separated into two terms by adopting the frozen permeability method. JMAG was utilized for this process. The two terms are the eddy current loss owing to the PM MMF and the eddy current loss owing to the armature MMF [6]. This process is graphically illustrated in Fig. 7. These separate eddy current losses of the rotor were estimated according to the stack length and motor volume. From the eddy current principle, the eddy current loss is proportional to the stack length and the square of the armature MMF [7]. This relationship can be expressed as (7) and (8)

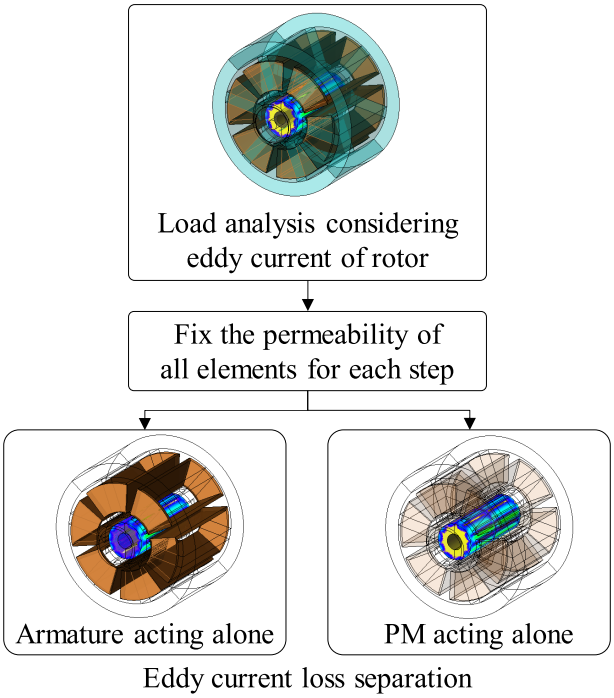

Fig. 7. Eddy current loss separation process.

owing to the armature and PM MMFs, respectively,

$$P_{\text{Eddy\_Arm.}} \propto L_{\text{stk}} \times (\text{MMF}_{\text{Arm.}})^2 \tag{7}$$

$$P_{\text{Eddy\_PM}} \propto L_{\text{stk}} \times (\text{MMF}_{\text{PM}})^2. \tag{8}$$

Combining (4) and (7), the eddy current loss due to the armature MMF for the modified model can be expressed as

$$\begin{aligned} P_{\text{Eddy\_Arm.}}^{\text{Modi.}} &= P_{\text{Eddy\_Arm.}}^{\text{Base}} \times \frac{L_{\text{stk}}^{\text{Modi.}} \times \left(\text{MMF}_{\text{Arm.}}^{\text{Modi.}}\right)^2}{L_{\text{stk}}^{\text{Base}} \times \left(\text{MMF}_{\text{Arm.}}^{\text{Base}}\right)^2} \\ &= P_{\text{Eddy\_Arm.}}^{\text{Base}} \times \frac{L_{\text{stk}}^{\text{Modi.}} \times \left(\text{MMF}_{\text{Arm.}}^{\text{Base}} \frac{L_{\text{stk}}^{\text{Base}}}{L_{\text{stk}}^{\text{Modi.}}}\right)^2}{L_{\text{stk}}^{\text{Base}} \times \left(\text{MMF}_{\text{Arm.}}^{\text{Base}}\right)^2} \\ &= P_{\text{Eddy\_Arm.}}^{\text{Base}} \times \frac{L_{\text{stk}}^{\text{Base}}}{L_{\text{stk}}^{\text{Modi.}}}. \end{aligned} \tag{9}$$

Similarly, by combining (5) and (8), the eddy current loss owing to the PM MMF can be expressed as

$$\begin{aligned} P_{\text{Eddy\_PM}}^{\text{Modi.}} &= P_{\text{Eddy\_PM}}^{\text{Base}} \times \frac{L_{\text{stk}}^{\text{Modi.}} \times \left(\text{MMF}_{\text{PM}}^{\text{Modi.}}\right)^2}{L_{\text{stk}}^{\text{Base}} \times \left(\text{MMF}_{\text{PM}}^{\text{Base}}\right)^2} \\ &= P_{\text{Eddy\_PM}}^{\text{Base}} \times \frac{L_{\text{stk}}^{\text{Modi.}} \times \left(\text{MMF}_{\text{PM}}^{\text{Base}}\right)^2}{L_{\text{stk}}^{\text{Base}} \times \left(\text{MMF}_{\text{PM}}^{\text{Base}}\right)^2} \\ &= P_{\text{Eddy\_PM}}^{\text{Base}} \times \frac{L_{\text{stk}}^{\text{Modi.}}}{L_{\text{stk}}^{\text{Base}}}. \end{aligned} \tag{10}$$

Thus, the eddy current loss of the modified model can be expressed as

$$P_{\text{Eddy}}^{\text{Modi.}} = P_{\text{Eddy\_Arm.}}^{\text{Base}} \times \frac{L_{\text{stk}}^{\text{Base}}}{L_{\text{stk}}^{\text{Modi.}}} + P_{\text{Eddy\_PM}}^{\text{Base}} \times \frac{L_{\text{stk}}^{\text{Modi.}}}{L_{\text{stk}}^{\text{Base}}}. \tag{11}$$

Using this simple estimation formula, the rotor eddy current loss can be estimated according to various motor sizes.

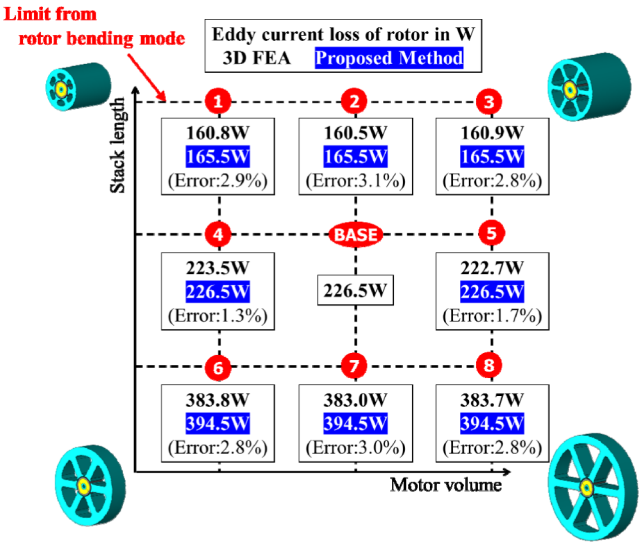

Fig. 8. Modified models and eddy current loss comparison between the 3-D FEA and the proposed method.

IV. Verification of the Proposed Estimation Method

Using the proposed estimation formula, eddy current losses were estimated according to the stack length. Furthermore, for a comparison, 3-D FEAs were conducted for several design points. From the model numbers 2 and 7 of Fig. 8, the error of the estimation result was less than 3.1%. Moreover, the model numbers 1, 4, 6, 3, 5, and 8 of Fig. 8 were verified with 3-D FEA for the validation of cases with different motor volumes. The errors of all the cases decreased and the maximum error was 2.9%. The boundary of the investigation was determined as a feasible design area considering the mechanical stability of the rotor. As the proposed method adopted the superposition principle to separate the eddy current loss due to armature and field, the magnetic nonlinearity of the stator core was not considered. Accordingly, it is estimated that the eddy current loss could not be perfectly separated. In addition, the end effects varying with the aspect ratio and load condition could affect the result [8], [9]. Even though there were some estimation errors, the proposed method allows the motor size to be determined considering the rotor eddy current loss. Especially, for the motor for which the proportion of the eddy current loss is large among the losses, the suggested method would be valuable.

V. Conclusion

This article proposed an estimation method for the rotor eddy current loss. The proposed method estimated the loss based on the 3-D FEA result of the base model. Using the frozen permeability method, the eddy current loss was separated into two terms: one from the armature MMF and the other from the PM MMF. Then, using the eddy current principle, a simple estimation formula was devised according to the stack length within the constraints. From this formula, eddy currents were estimated for various motor sizes and compared with the results of 3-D FEA. The maximum error was 3.1%. Overall, the method proposed in this article is expected to be useful in determining the UHS motor size.

ACKNOWLEDGMENT

This research was supported in part by the Ministry of Trade, Industry, and Energy (MOTIE), Korea, under the "Commercializing fuel cell electric vehicle component industry and R&D Support Program" under Reference R0006468 supervised by the Korea Institute for Advancement of Technology (KIAT).

REFERENCES

[1] B. Hannon, P. Sergeant, and L. Dupre, "Evaluation of the rotor eddy-current losses in high-speed PMSMs with a shielding cylinder for different stator sources," *IEEE Trans. Magn.*, vol. 55, no. 3, pp. 1–10, Mar. 2019.

[2] Z. Zhang, Z. Deng, Q. Sun, C. Peng, Y. Gu, and G. Pang, "Analytical modeling and experimental validation of rotor harmonic eddy-current loss in high-speed surface-mounted permanent magnet motors," *IEEE Trans. Magn.*, vol. 55, no. 2, pp. 1–11, Feb. 2019.

[3] M.-S. Lim, S.-H. Chai, J.-S. Yang, and J.-P. Hong, "Design and verification of 150-krpm PMSM based on experiment results of prototype," *IEEE Trans. Ind. Electron.*, vol. 62, no. 12, pp. 7827–7836, Dec. 2015.

[4] R. G. Budynas, *Shigleys Mechanical Engineering Design*. New York, NY, USA: McGraw-Hill, 2011.

[5] J.-H. Sim, D.-Y. Kim, S.-I. Kim, and J.-P. Hong, "Analytical electromagnetic modeling and experimental validation of vehicle horn considering skin effect in its solid cores," *IEEE Trans. Magn.*, vol. 53, no. 6, pp. 1–4, Jun. 2017.

[6] D.-G. Ahn, M.-H. Yoon, J.-P. Hong, and J.-W. Jung, "Finite-element analysis of local flux density variation considering PWM current harmonics," *IEEE Trans. Magn.*, vol. 54, no. 3, pp. 1–4, Mar. 2018.

[7] S. Steentjes, S. Boehmer, and K. Hameyer, "Permanent magnet eddy-current losses in 2-D FEM simulations of electrical machines," *IEEE Trans. Magn.*, vol. 51, no. 3, pp. 1–4, Mar. 2015.

[8] J.-W. Jung, H.-I. Park, J.-P. Hong, and B.-H. Lee, "A novel approach for 2-D electromagnetic field analysis of surface mounted permanent magnet synchronous motor taking into account axial end leakage flux," *IEEE Trans. Magn.*, vol. 53, no. 11, pp. 1–4, Nov. 2017.

[9] Y. Chen, Z. Q. Zhu, and D. Howe, "Three-dimensional lumped-parameter magnetic circuit analysis of single-phase flux-switching permanent-magnet motor," *IEEE Trans. Ind. Appl.*, vol. 44, no. 6, pp. 1701–1710, Nov. 2008.